

A ~ 43 GeV γ -ray line signature in the directions of a group of nearby massive galaxy clusters

Yi-Zhong Fan,^{1,2,*} Zhao-Qiang Shen,^{1,†} Yun-Feng Liang,^{3,‡} Xiang Li,^{1,2,§}
Kai-Kai Duan,¹ Zi-Qing Xia,¹ Xiao-Yuan Huang,^{1,2} Lei Feng,^{1,2} and Qiang Yuan^{1,2}

¹Key Laboratory of Dark Matter and Space Astronomy,

Purple Mountain Observatory, Chinese Academy of Sciences, Nanjing 210023, China

²School of Astronomy and Space Science, University of Science and Technology of China, Hefei, Anhui 230026, China

³Guangxi Key Laboratory for Relativistic Astrophysics,

School of Physical Science and Technology, Guangxi University, Nanning 530004, China

(Dated: July 17, 2024)

As the largest gravitationally bound objects in the Universe, galaxy clusters have provided the first piece of evidence for the presence of dark matter and may be suitable targets for indirect dark matter searches. Among various signals, the GeV-TeV γ -ray line has been taken as the smoking-gun signal of the dark matter annihilation/decay since no known astrophysical/physical process(es) could generate such a peculiar spectrum. With 15.5 years of Fermi-LAT P8R3 publicly available data, we search for the γ -ray line emission in the directions of a group of 13 nearby massive galaxy clusters with an unbinned likelihood analysis. A γ -ray line signal at ~ 43.2 GeV has a net TS value of ≈ 30 if we only take into account the data in the directions of Virgo, Fornax and Ophiuchus clusters, three massive clusters with the highest J-factors expected to generate the dark matter annihilation signal. The signal still presents when the data of other 10 nearby massive clusters have also been included, though the TS value decreases to ≈ 21 likely because of their lower signal-to-noise ratios. The absence of this signal in the inner Galaxy disfavors both the instrumental effect and the canonical dark matter annihilation interpretation, and a more sophisticated dark matter model or very peculiar astrophysical scenario might be needed. This γ -ray line signal, if intrinsic, could be unambiguously verified by the Very Large Area γ -ray Space Telescope in its first two years of performance.

I. INTRODUCTION

The observations of various gravitational phenomena at different scales strongly suggest the presence of dark matter (DM) [1]. Many interesting dark matter particle candidates have been proposed in the literature, and the weakly interacting massive particles (WIMPs) are the leading ones since they can naturally explain today's relic density of DM [2]. The WIMPs may annihilate with each other or decay, and finally generate stable standard model particle pairs, such as the gamma rays, the neutrinos and antineutrinos, electrons and positrons, protons and antiprotons, and so on. The successful identification of such signals in turn can be used to infer the properties of the dark matter particles. Though dedicated efforts have been made in the passed decades, no confidential dark matter signal has been identified in either gamma rays or cosmic rays [3–8]. One challenge is that the resulting energy spectra of the products are usually smooth, so it is hard to distinguish them from astrophysical backgrounds [2, 3]. The situation could change if the products have a sharp structure like a line, as expected in the annihilation or decay of WIMPs χ into a two-body final state $\gamma\chi$ [9] (or the decay of the gravitinos through

$\chi \rightarrow \gamma\nu$ [10]). The line energy is $E_\gamma = m_\chi(1 - m_X^2/4m_\chi^2)$ for dark matter annihilation, where X could be either γ , Z_0 or h_0 , depending on the mass of the dark matter particle [9, 11].

Shortly after the first release of the Fermi-LAT data, quite a few groups searched for γ -ray line signals in the directions of the inner Galaxy and did find evidence for the presence of ~ 130 GeV line [12–15]. Such a signal, however, turns out to be a systematic effect of the early data reconstruction of Fermi-LAT [16–18]. This null result has also been confirmed by the independent observation of the DARK MATTER PARTICLE EXPLORER (DAMPE) [19, 20]. With the Pass 8 data of Fermi-LAT, we have concentrated on the galaxy clusters, the most massive gravitational bound systems in the Universe and contain a large number of substructures that may be promising targets for dark matter search [21, 22], and found hint for a ~ 43 GeV γ -ray line in the direction of a group of nearby massive galaxy clusters [23, 24]. In this work we show that this signal still presents in the latest data and its significance, though characterized by a sizable drop around MJD 57500, grows up again at late times. If intrinsic, this signal will be unambiguously verified by the Very Large Area γ -ray Space Telescope (VLAST), a MeV-TeV detector distinguished by a peak acceptance of ~ 12 m² sr and an excellent energy resolution of $\sim 1.3\%$ at 50 GeV, which has been proposed by some DAMPE people [25], in $\sim 1 - 2$ years of performance.

* yzfan@pmo.ac.cn

† zqshen@pmo.ac.cn

‡ liangyf@gxu.edu.cn

§ xiangli@pmo.ac.cn

II. METHODOLOGY

The sample of galaxy clusters. Our baseline sample consists of 13 galaxy clusters with large J-factors, most were selected from the extended HIFLUGCS catalog [26, 27], which are basically the same as that used in Liang et al. [23], except that we remove Perseus because of its strong gamma-ray activity, and 3C129 as well as A3627 for their low attitudes/high background (though Ophiuchus is also at a low altitude, it's J-factor is large and the expected signal-to-noise ratio is still reasonably high). The region of the interest (ROI) for each galaxy cluster is defined with the angular radius $\theta_{200} = \arctan(R_{200}/d_A)$, where d_A is the angular diameter distance and R_{200} is the corresponding virial radius. In our analysis, the overlapped region of Virgo and M49 is only taken into account once. Please see Table I in Appendix A for a summary of our sample.

The γ -ray data. We take the Fermi-LAT P8R3_V3 data based on the most recent event-level analysis, which alleviates the background cosmic rays leaked from the ribbons of the anticoincidence detector [28]. The ULTRACLEAN events are adopted to reduce the cosmic-ray contamination [29]. We only take into account the EDISP1+EDISP2+EDISP3 data, collected between 2008 October 27 and 2024 May 2 (Fermi Mission Elapsing Time between 246823875 and 736304518), since the energy resolution of the EDISP0 data is significantly worse than the other events [30]. We further select the events with zenith angles less than 90° and apply the quality filter cut (`DATA_QUAL==1`) && (`LAT_CONFIG==1`).

The unbinned likelihood line search method. We perform an unbinned likelihood analysis, employing a sliding-window technique and splitting the analysis into a series of energy windows, to search for spectral lines [12, 13, 16, 23, 29]. We consider a series of line energies E_{line} from 5 GeV to 300 GeV with $0.5\sigma_E$ energy steps where σ_E is the 68% instrument energy resolution. Each energy window has a width of $[0.5E_{\text{line}}, 1.5E_{\text{line}}]$. Within each window, the unbinned likelihood fit is carried out by assuming a power-law background. The small width of the energy window ensures the power-law function as a good approximation to the background spectrum. The observational data towards the galaxy clusters are fitted with both null (purely power law) and signal (power law plus a line component) models.

The likelihood for the null model is expressed as

$$\ln\mathcal{L}_{\text{null}}(\Theta_b) = \sum_{i=1}^{N_{\text{gcl}}} \ln [F_b(E_i; \Theta_b)\bar{\epsilon}(E_i)] - \int F_b(E; \Theta_b)\bar{\epsilon}(E)dE, \quad (1)$$

where N_{gcl} is the number of clusters in the analysis, E_i is the energy of each Fermi-LAT photon within ROI, F_b is the power-law background spectrum and Θ_b represents the nuisance parameters of the background. For the sig-

nal model, the likelihood is

$$\ln\mathcal{L}_{\text{sig}}(N_s, E_{\text{line}}, \Theta_b) = \sum_{i=1}^{N_{\text{gcl}}} \ln [(F_b(E_i; \Theta_b)\bar{\epsilon}(E_i) + F_s(E_i)\bar{\epsilon}(E'_{\text{line}}))] - \int [F_b(E; \Theta_b)\bar{\epsilon}(E) + F_s(E)\bar{\epsilon}(E'_{\text{line}})]dE, \quad (2)$$

with $F_s(E) = N_s\bar{D}(E; E'_{\text{line}})$ the line component at an observed line energy of E'_{line} and $\bar{D}(E; E'_{\text{line}})$ the exposure-averaged instrument energy dispersion. The $\bar{\epsilon}$ is the instrument exposure averaged over the entire ROI. For details of the calculation of the energy dispersion $\bar{D}(E; E'_{\text{line}})$, please see Ref. [23]. To improve the line search sensitivity, we take into account the redshifts of the clusters by using $E'_{\text{line}} = E_{\text{line}}/(1+z)$, where E_{line} is the source-frame energy of the line produced in the cluster at the redshift of z . During the analysis, the minimization of the likelihood is implemented by the Python package `iminuit` [31].

A test statistic (TS) is defined as $\text{TS} \equiv 2 \ln(\hat{\mathcal{L}}_{\text{sig}}/\hat{\mathcal{L}}_{\text{null}})$, where $\hat{\mathcal{L}}$ is the best-fit likelihood value. The local significance of a line signal can be approximated as the square root of the TS value. A more accurate/realistic estimation of the global significance will be obtained through Monte Carlo (MC) simulations (see Sec. IV C).

III. RESULTS AND DISCUSSIONS

A. The signature in the spectra of the stacked galaxy clusters

Figure 1 presents the spectral properties of the stacked galaxy clusters. The upper panel is for the spectral energy distributions (SEDs) of the three galaxy clusters with the largest J-factors (the data points in blue) and the whole sample (the data points in black). The SED is defined as $(dN/dE)_j = \sum_{i=1}^{N_{\text{gcl}}} n_{ij}/(\bar{\epsilon}_j \Delta E_j \sum_{i=1}^{N_{\text{gcl}}} \Omega_i)$, where Ω_i is the solid angle and n_{ij} is the photon number at the energy bin E_j for the i -th cluster. Clearly, a distinct spike displays in both spectra, though for the whole sample the signal is relatively weaker. This is likely attributed to its higher background in comparison to the case of the first three galaxy clusters.

We then carry out the unbinned likelihood line search (i.e., the sliding-window data analysis). The results are reported in the lower panel of Figure 1 and the TS value reaches 30.1 (21.3) for the first three galaxy clusters (the whole sample). The derivation of the global significance via the random sky simulations is detailed in Appendix IV C. It turns out that for the signal in the whole sample the global significance is about 3.7σ , while for the three galaxy clusters with the largest J-factors the global significance is about 4.3σ . We have also carried out the same line search procedure for the earth limb data above 10 GeV whose zenith angles are within $111^\circ - 113^\circ$

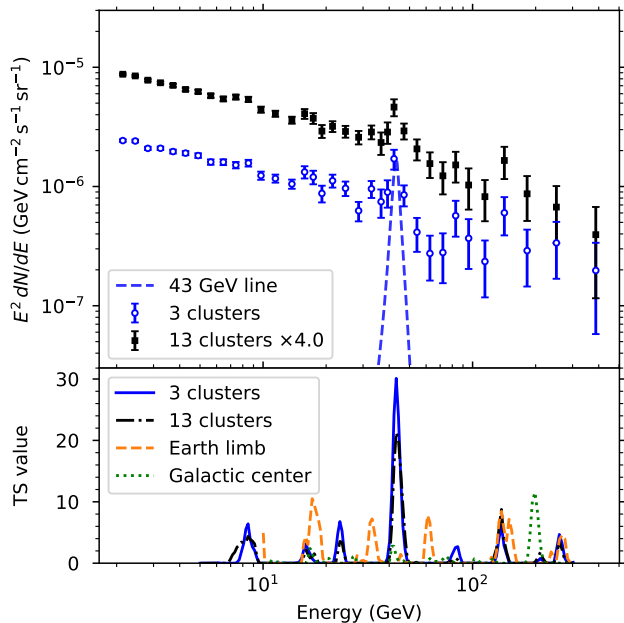


FIG. 1. The upper panel is for the spectral energy distributions (SEDs) of the three galaxy clusters with the largest J-factors (the blue points) and the whole sample (the black points). The lower panel shows the corresponding test statistic values of the possible γ -ray line signal in the directions of the first three galaxy clusters (the blue line), the whole sample (the dotted-dashed black line), as well as the null result from the earth limb (the dashed orange line) and the 3° region around Galactic center (green dotted line).

and rocking angles are $> 52^\circ$ [16, 23, 32], and found a null result (see the dashed orange line in the lower panel of Figure 1). We have searched for lines in the inner 3° region around the Galactic center and found no signal as well (green dotted line). Together with the non-detection in the inner Galaxy data [20], we find no evidence for a systematic error origin of our signal.

Figure 2 provides the details of the TS evolution of the signal. In the left panel, we present the TS value of the line signal in the direction of each ROI and the evolution of the net TS value of a group of sources as the sources accumulate. The order of the galaxy clusters is based on their J-factors (without considering the possible boost factor, see Table I in the Appendix). No signal is detected in the direction of M49. This likely indicates a small boost factor because the dark matter distribution substructures may be atypical in view of that M49 may have even already passed through Virgo once, as revealed by the extended X-ray study [33]. The right panel of Figure 2 displays the time evolution of the TS values of the three galaxy clusters (the blue line) as well as the whole sample (the black dashed line). For the former, the net TS value roughly increases with time, though strong fluctuation is displayed in the time interval of MJD 57000-59000. While for the whole sample, the net TS value peaks at about MJD 57700. After that

there came a quick drop of the TS value. Since MJD 58600, the TS value has been increasing again. Roughly, the TS values of the signal in the directions of Virgo and Ophiuchus increase with time linearly, indicating a stable emission process.

B. Stringent constraints on the canonical dark matter origin of the γ -ray line signal

It is widely believed that the inner Galaxy would have the brightest dark matter annihilation signal. In the canonical dark matter model, strong line emission would be expected from the inner Galaxy if the signal in the directions of the galaxy clusters is intrinsic. The null results, as widely reported [16, 20], are against the instrumental effect origin of the 43 GeV γ -ray line signal. The stringent upper limits are reported in Figure 3. Clearly, the non-detection of the ~ 43 GeV line signal in the inner Galaxy region is strongly in tension with that of the galaxy clusters. There are some possible solutions. One is that the substructures of the galaxy clusters are so rich that their boost factors of the dark matter annihilation are high up to $\sim 10^3$. Such a possibility, though believed possible in some literature [21], is not supported by the more recent numerical simulations [34–36]. The other possibility is that the canonical model [37] is too simple and the real situation is much more complicated. In a recent systematic study of velocity-dependent dark matter annihilation (including the Sommerfeld enhancement) in a variety of astrophysical objects, it was found that for s -wave on resonances and for p -wave in the no-Sommerfeld enhancement regime the galaxy clusters can outshine all other classes of targets [38]. The non-detection of the continual emission component in the direction of Virgo imposes an additional challenge (see the Appendix). Another possibility is that the ~ 43 GeV line signal has an astrophysical origin and hence is irrelevant to the dark matter. One model, initially motivated by the 130 GeV signal reported in the inner Galaxy, is that the Comptonization of a cold ultrarelativistic, but mono-energetic, electron-positron pulsar wind in the deep Klein-Nishina regime can yield narrow (with a width ≤ 0.2) distinct γ -ray line features [39]. Though interesting, it seems challenging to realize such a specific scenario in the galaxy clusters.

C. Prospect of testing the ~ 43 GeV γ -ray line signal with VLAST

Fermi-LAT is in good condition and the continual excellent performance provides the guarantee of collecting more high-quality data, which will be crucial to test whether the ~ 43 GeV signal is real or not. Nevertheless, the double of the current data can only be achievable until 2040. Fortunately, the next generation γ -ray space telescopes are in proposal. VLAST, a Chinese space mis-

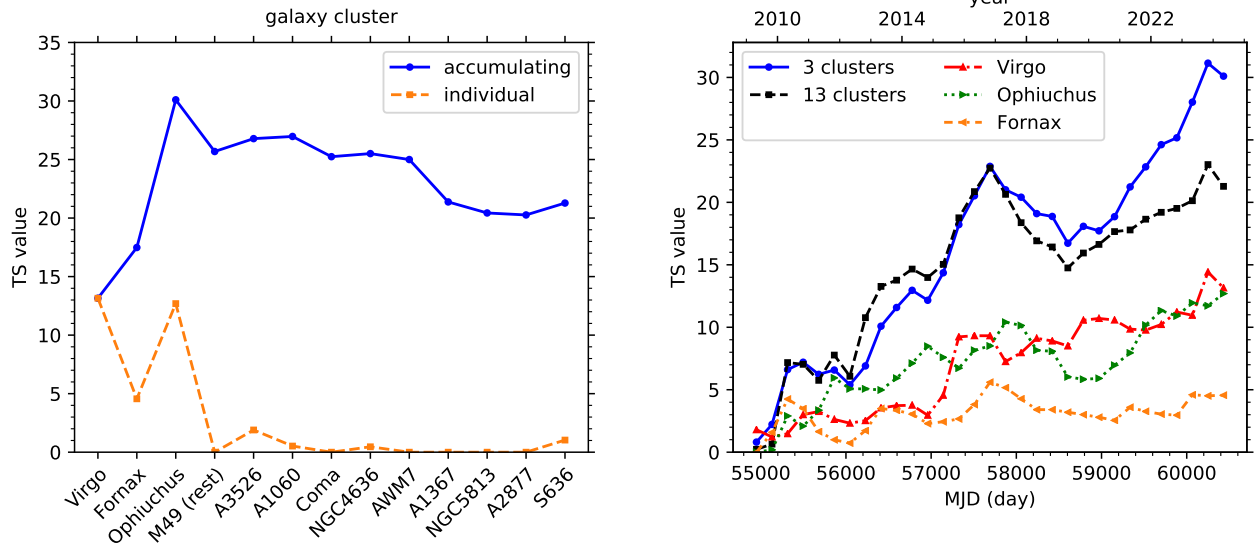


FIG. 2. The left panel is for the TS value of the line signal in the direction of each galaxy cluster (the orange line) and the evolution of the net TS value of a group of sources with the accumulation of sources (the blue line). The right panel is for the time evolution of the TS values of the three galaxy clusters (the blue line), the whole sample (the black dashed line) as well as the individual clusters of Virgo (the red dot-dashed line), Ophiuchus (the green dotted line) and Fornax (the orange dot-dot-dashed line).

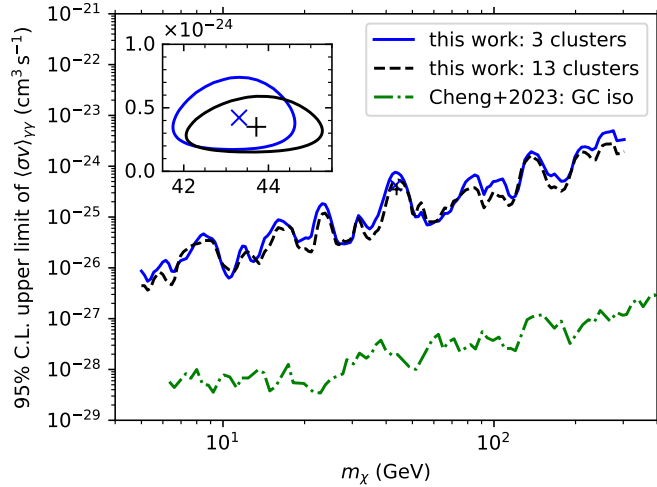


FIG. 3. The inset shows the best-fit parameters needed in the dark matter annihilation origin of the ~ 43 GeV signal, note that the boost factors of the galaxy clusters have not been taken into account. At other energies, we present upper limits. The upper limits set by the null signals in the inner Galaxy [20] are shown for comparison.

sion being proposed, is characterized by a large acceptance of $\sim 12 \text{ m}^2 \text{ sr}$ at GeV-TeV energies and an excellent energy resolution of $\sim 1.3\%$ at 50 GeV [25]. Given the high acceptance/energy-resolution, such a telescope will be wonderful to clarify whether there is a distinct γ -ray line from the galaxy clusters. We have simulated 2-yr VLAST observations of the 13 galaxy clusters (see Fig-

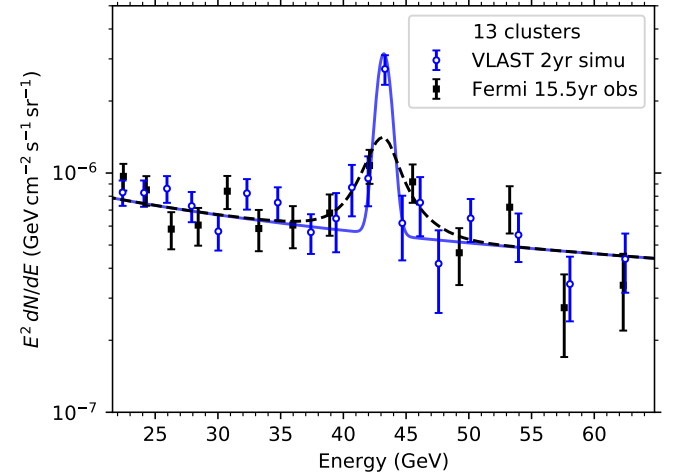


FIG. 4. The SED of the 2-yr VLAST simulation of the 13 galaxy clusters (the blue points) in the energy window around 43 GeV. The blue solid line is the input model based on the best-fit spectral parameters of the Fermi-LAT observation. The black points and the black dashed line are the Fermi-LAT SED and the fitted spectrum, respectively.

ure 4), adopting the best-fit results of the signal as well as the background for the current Fermi-LAT data as the input, where the VLAST instrumental response functions are taken from [25]. The TS value of the 43 GeV line is expected to be ~ 73 . Therefore, the successful performance of VLAST in $\sim 1 - 2$ years will be sufficient to confirm the presence of the line signal if the current

Fermi-LAT signal is intrinsic.

IV. CONCLUSION

We have analyzed the 15.5-yr observation data of Fermi-LAT in the directions of a group of nearby very-massive galaxy clusters. With an unbinned likelihood approach, we find a γ -ray line signal at ~ 43.2 GeV. In particular, if we only take into account the data in the directions of Virgo, Fornax and Ophiuchus clusters, three massive clusters with the highest J-factors, the net TS value is ≈ 30 , corresponding to a global significance of 4.3σ . The signal still presents for the whole sample, though the TS value decreases to ≈ 21 , corresponding to a global significance of 3.7σ , likely because of the lower signal-to-noise ratios for other sources. The absence of this signal in both the inner Galaxy and the Earth limb disfavors an instrumental origin. Anyhow, the canonical dark matter annihilation interpretation is challenged by the stringent constraints set by the inner Galaxy and it is unclear whether there could be a peculiar astrophysical origin. Besides investigating its possible physical origin, it is urgent to clarify the robustness of this signal. Dark Matter Particle Explorer (DAMPE) also works in this energy range and has an excellent energy resolution. But its acceptance is smaller than Fermi-LAT by a factor of ~ 7 [40]. The expected detection prospect of the line signal is low, consistent with the null result found in the analysis of the DAMPE data (see Appendix IV D). If the 43 GeV γ -ray line is indeed intrinsic, till 2040 the Fermi-LAT data will be doubled and the signal will be confirmed. A quicker independent test is also possible. For the VLAST proposed by some DAMPE people, a robust clarification is expected in the first two years of its performance.

ACKNOWLEDGMENTS

This work was supported in part by the National Key Research and Development Program of China (No. 2022YFF0503301 and No. 2022YFF0503304), the Project for Young Scientists in Basic Research of the Chinese Academy of Sciences (No. YSBR-092 and No. YSBR-061), the New Cornerstone Science Foundation through the XPLOER PRIZE, and the National Natural Science Foundation of China (No. 11921003, No. U1738210, No. 12220101003, No. 12003074, and No. 12003069).

APPENDIX

A. The sample of the galaxy clusters

In Table I we summarize the parameters of the target galaxy clusters. For Virgo we take $R_{200} = 0.974$ Mpc [41]. A larger R_{200} has been suggested in recent literature [42], but the dark matter beyond such a radius needs to be tiny, which is hard to be understood in the Λ CDM paradigm. Ophiuchus is the second brightest galaxy cluster in X-ray band. Because of its low latitude, the optical data are still poor and the inferred density profile in optical is significantly different from that measured in infrared band [43], therefore in this work we take the R_{200} derived in X-rays [27].

B. The search for the possible continual emission component associated with the line signal

Theoretically, dark matter annihilation to photons is loop-suppressed, and it is expected to predominantly annihilate through quark and charged-lepton channels. Therefore, if the ~ 43 GeV γ -ray line signal analyzed in this paper is indeed produced by dark matter, it would be accompanied by a continual γ -ray component generated from dark-matter annihilation to quarks or charged leptons. Here we attempt to search for such a continual-spectrum signal. Our analysis primarily targets at the Virgo cluster, which has the highest expected J-factor. We performed a standard Fermi-LAT binned likelihood analysis using a $20^\circ \times 20^\circ$ ROI with a bin size of 0.1° . The background model includes all 4FGL-DR4 sources [46] and two large-scale diffuse components (the Galactic interstellar emission and isotropic diffuse component). We add a dark matter component into the background model to examine the existence of the continual emission, with its spatial template derived from considering an NFW density distribution. The related parameters r_s and ρ_0 are given by M_{200} and R_{200} listed in Table I. We consider two representative annihilation channels, $b\bar{b}$ and $\tau^+\tau^-$, with the corresponding annihilation spectra generated with PPPC4DMID [47].

For our purpose, we fix the DM mass at 43.2 GeV, the best-fit mass of the top three clusters in Fig. 3. We do not detect any significant continual γ -ray emission beyond the background of dark-matter annihilation for both the $b\bar{b}$ and $\tau^+\tau^-$ channels, with the TS values approximately 0. Therefore, we place the upper limits on the annihilation cross section $\langle\sigma v\rangle$ of dark matter to these two final states. The results are shown in Fig. 5. For comparison, also plotted in the figure are the constraints given by Fermi-LAT observations of dwarf spheroidal galaxies [48, 49], which generally represent the strongest limits on the dark matter annihilation cross-section in this mass range. We have also plotted the upper limits that assumed an optimistic boost factor of 1299 (such a large boost factor is probably necessary to ensure that the ~ 43

TABLE I. Parameters of the GClS. The redshift z , right ascension α and declination δ in J2000 epoch of each GCl are taken from [27]. The virial radii R_{200} and virial masses M_{200} are taken from the references [33, 41, 44] for Virgo, M49 and S636 respectively. For the other clusters, the masses and radii are converted from R_{500} tabulated in [27]. The concentration c_{200} of Virgo is from the observation [41], while for the others the concentration-mass relation in [34] is adopted. θ_{200} is the angular size of R_{200} , $J_{\text{NFW}} \equiv \int_{\Omega_{200}} \int_{\text{los}} \rho_{\text{NFW}}^2(r(l)) dl d\Omega$ is the J-factor given the NFW profile of the clusters, and $b_{\text{sh},\text{M17}}$ is the boost factor within R_{200} parameterized in [35] for the subhalo mass function with the slope of 2. The following cosmological parameters are used: $H_0 = 73.6 \text{ km s}^{-1} \text{ Mpc}^{-1}$, $\Omega_{\text{M}} = 0.334$ and $\Omega_{\Lambda} = 0.666$ [45]. The three clusters below the horizontal line are those contained in the previous works [22–24] but excluded in this work due to the high background emission.

GCl	α (deg)	δ (deg)	z	M_{200} ($10^{14} M_{\odot}$)	R_{200} (Mpc)	c_{200}	θ_{200} (deg)	$\log_{10}(J_{\text{NFW}})$ ($\text{GeV}^2 \text{ cm}^{-5}$)	$b_{\text{sh},\text{M17}}$
Virgo	187.704	12.391	0.0038	1.050	0.926	8.80	3.47	18.396	47.80
Fornax	54.669	-35.310	0.0046	1.196	0.981	5.48	3.02	17.906	48.53
Ophiuchus	258.111	-23.363	0.0280	34.691	2.991	4.98	1.56	17.769	67.34
M49	187.444	7.997	0.0038	0.460	0.704	5.84	2.62	17.720	43.27
A3526	192.200	-41.309	0.0103	3.156	1.354	5.20	1.87	17.600	54.06
A1060	159.178	-27.521	0.0114	2.309	1.219	5.28	1.53	17.388	52.27
Coma	194.947	27.939	0.0232	9.004	1.911	5.01	1.19	17.344	60.05
NGC4636	190.708	2.688	0.0037	0.155	0.497	6.35	1.90	17.313	37.65
AWM7	43.623	41.578	0.0172	4.491	1.519	5.12	1.27	17.308	56.08
A1367	176.190	19.703	0.0216	6.733	1.736	5.05	1.16	17.283	58.40
NGC5813	225.299	1.698	0.0064	0.385	0.672	5.92	1.49	17.184	42.32
A2877	17.480	-45.922	0.0241	6.166	1.684	5.06	1.01	17.155	57.90
S636	157.421	-35.326	0.0093	0.763	0.844	5.64	1.29	17.124	46.03
A3627	243.555	-60.843	0.0163	4.487	1.519	5.12	1.34	17.353	56.08
Perseus	49.946	41.515	0.0183	5.476	1.622	5.08	1.28	17.337	57.22
3C129	72.560	45.026	0.0223	4.796	1.550	5.11	1.00	17.117	56.46

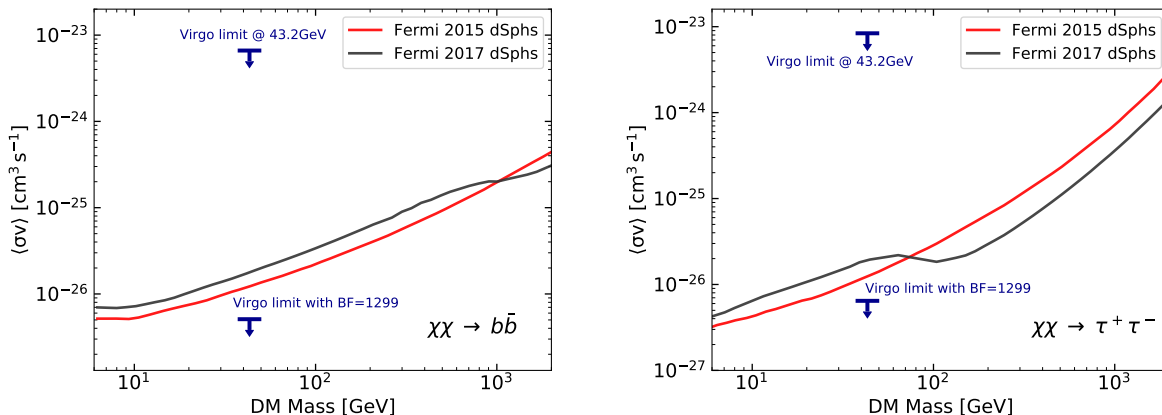


FIG. 5. Theoretically, if the ~ 43 GeV line signal is true, it is expected to be accompanied by continuous γ -ray emission from the DM annihilation to quarks or charged leptons. We search for such emission toward the Virgo cluster and find no signal. Upper limits on $\langle\sigma v\rangle$ at a DM mass of 43.2 GeV are therefore placed. We also plot the upper limits assuming an optimistic boost factor of 1299 for Virgo.

GeV line signal does not conflict with the line search results from the observations of the Galactic center region [19, 20]). It can be seen that under this choice of boost factor, the dark matter cross-section is constrained to a very low value, which may impose challenges for model building if the line signal is true.

C. The trail factors of the line signal

Since multiple trials were adopted to search for the largest TS values, the “look elsewhere effect” should be considered. To estimate the global significance, we performed the random sky simulations [50]. In each simula-

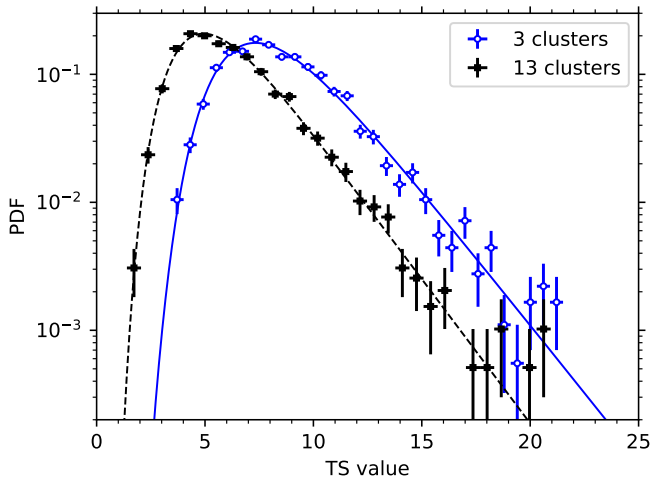


FIG. 6. The distributions of the maximal TS values of 3000 random sky simulations for the whole sample (the black points) and the first three galaxy clusters (the blue points). The lines are the best-fit trial-corrected χ^2 distribution.

tion, 13 regions were selected randomly in the sky with the radii aligned with the galaxy clusters. We excluded those around the Galactic plane ($|b| < 5^\circ$) or the Galactic center ($|l| < 20^\circ$ and $|b| < 9^\circ$), or close to the strong point sources ($F_{1000} > 2 \times 10^{-9}$ ph cm $^{-2}$ s $^{-1}$ in the 4FGL-DR4 catalog [46]). In total 3000 random ROI sets were generated.

For the whole sample, the trials over the line energies should be taken into account. We carried out the same sliding windows analyses using all the 13 random regions in the each simulation and recorded the largest TS value. The TS value distribution is shown with the black points in Figure 6. We fit the distribution with the trial-corrected χ^2 distribution, whose cumulative distribution function is assumed to be $P_g(\text{TS} < c; k, t) = [P(\chi_k^2 < c)]^t$ [13]. The best-fit trial factor is $t = 25 \pm 5$ and the degree of freedom is $k = 1.30 \pm 0.15$. The global significance is $\approx 3.7\sigma$ given the local TS value of 21.3.

For the first three galaxy clusters, there is another trial over the number of analyzed sources. In each simulation, we derive the accumulative TS values for gradually increasing samples whose ROIs follow those of target clusters. The largest TS value among all the fittings in each simulation is collected and the final distribution is shown in blue in Figure 6. The best-fit parameters of the trial-corrected χ^2 distribution are $t = 22 \pm 3$ and $k = 2.59 \pm 0.18$. Therefore, the TS value of 30.1 corresponds to a global significance of $\approx 4.3\sigma$.

D. The DAMPE data

DAMPE is a pair-conversion γ -ray telescope with an excellent energy resolution [19]. Utilizing the pub-

licly available six years (<https://dampe.nssdc.ac.cn/>

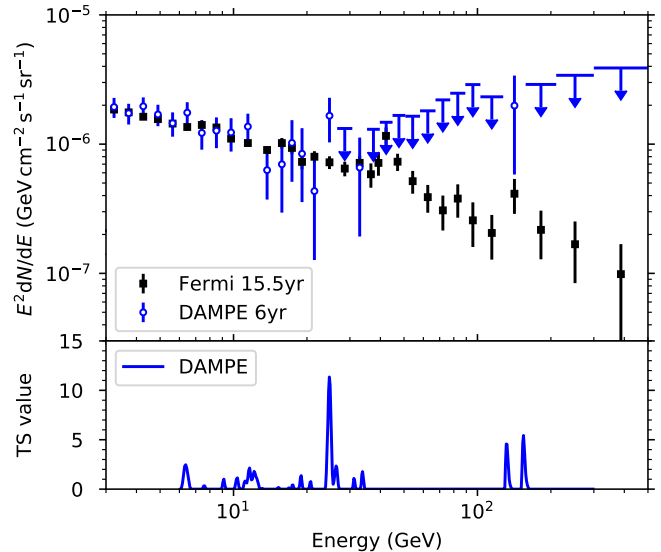


FIG. 7. The upper panel demonstrates the stacked SED of the 13 galaxy clusters observed by DAMPE (the blue points) and Fermi-LAT (the black points). Upper limits are presented if the photon count within the energy bin is less than two. The lower panel shows the TS values of γ -ray lines by analyzing the DAMPE data.

dampe/mission.php) of High-Energy-Trigger DAMPE photon data [51], we searched for the line signal in the sample of 13 galaxy clusters. The DmpST package [52] is employed in the analysis.

We selected photons with energy ≥ 3 GeV from the 13 clusters within the radii of θ_{200} and calculated the stacked SED. In the calculation, we considered the ϕ -dependence of the effective area due to the nonuniform exposure. As depicted in the upper panel of Figure 7, the flux from the DAMPE (blue points) is well consistent with that of the Fermi-LAT (black points). Owing to the small acceptance of DAMPE, no photon is detected between 34 GeV and 130 GeV and the flux upper limits are drawn.

The unbinned sliding windows analysis was adopted to search for the line signal above 6 GeV. No significant γ -ray lines are found by DAMPE as shown in the lower panel of Figure 7, especially the TS value at ~ 43 GeV is zero. Based on the best-fit parameters in the Fermi-LAT sliding windows analysis, the expected photon number of the line is found to be 1.53. It is 21.6% in probability for zero detected photon within the energy bin of 42 – 44 GeV. Therefore, the null result based on the DAMPE data is still consistent with the result of Fermi-LAT.

-
- [1] G. Bertone and D. Hooper, *Reviews of Modern Physics* **90**, 045002 (2018), arXiv:1605.04909 [astro-ph.CO].
- [2] J. L. Feng, *Ann. Rev. Astron. Astrophys.* **48**, 495 (2010), arXiv:1003.0904 [astro-ph.CO].
- [3] E. Charles, M. Sánchez-Conde, B. Anderson, R. Caputo, *et al.*, *Phys. Rep.* **636**, 1 (2016), arXiv:1605.02016 [astro-ph.HE].
- [4] J. Conrad and O. Reimer, *Nature Physics* **13**, 224 (2017), arXiv:1705.11165 [astro-ph.HE].
- [5] Y.-Z. Fan, T.-P. Tang, Y.-L. S. Tsai, and L. Wu, *Phys. Rev. Lett.* **129**, 091802 (2022), arXiv:2204.03693 [hep-ph].
- [6] H. Abdalla *et al.* (H.E.S.S.), *Phys. Rev. Lett.* **129**, 111101 (2022), arXiv:2207.10471 [astro-ph.HE].
- [7] H. Abe *et al.* (MAGIC), *Phys. Rev. Lett.* **130**, 061002 (2023), arXiv:2212.10527 [astro-ph.HE].
- [8] Z. Cao *et al.* (LHAASO), *Phys. Rev. Lett.* **in press**, arXiv:2406.08698 [astro-ph.HE].
- [9] L. Bergström and H. Snellman, *Phys. Rev. D* **37**, 3737 (1988).
- [10] A. Ibarra and D. Tran, *Phys. Rev. Lett.* **100**, 061301 (2008), arXiv:0709.4593 [astro-ph].
- [11] S. Rudaz and F. W. Stecker, *Astrophys. J.* **368**, 406 (1991).
- [12] T. Bringmann, X. Huang, A. Ibarra, S. Vogl, and C. Weniger, *J. Cosmol. Astropart. Phys.* **2012**, 054 (2012), arXiv:1203.1312 [hep-ph].
- [13] C. Weniger, *J. Cosmol. Astropart. Phys.* **2012**, 007 (2012), arXiv:1204.2797 [hep-ph].
- [14] E. Tempel, A. Hektor, and M. Raidal, *J. Cosmol. Astropart. Phys.* **2012**, 032 (2012), arXiv:1205.1045 [hep-ph].
- [15] M. Su and D. P. Finkbeiner, *ArXiv e-prints* (2012), arXiv:1206.1616 [astro-ph.HE].
- [16] M. Ackermann, M. Ajello, A. Albert, B. Anderson, *et al.* (Fermi-LAT), *Phys. Rev. D* **91**, 122002 (2015), arXiv:1506.00013 [astro-ph.HE].
- [17] S. Li, Z.-Q. Xia, Y.-F. Liang, K.-K. Duan, Z.-Q. Shen, X. Li, L. Feng, Q. Yuan, Y.-Z. Fan, and J. Chang, *Phys. Rev. D* **99**, 123519 (2019), arXiv:1806.00733 [astro-ph.HE].
- [18] P. De La Torre Luque, J. Smirnov, and T. Linden, *Phys. Rev. D* **109**, L041301 (2024), arXiv:2309.03281 [hep-ph].
- [19] F. Alemanno *et al.* (DAMPE), *Sci. Bull.* **67**, 679 (2022), arXiv:2112.08860 [astro-ph.HE].
- [20] J.-G. Cheng, Y.-F. Liang, and E.-W. Liang, *Phys. Rev. D* **108**, 063015 (2023), arXiv:2308.16762 [astro-ph.HE].
- [21] L. Gao, C. S. Frenk, A. Jenkins, V. Springel, and S. D. M. White, *Mon. Not. R. Astron. Soc.* **419**, 1721 (2012), arXiv:1107.1916 [astro-ph.CO].
- [22] B. Anderson, S. Zimmer, J. Conrad, M. Gustafsson, M. Sánchez-Conde, and R. Caputo, *J. Cosmol. Astropart. Phys.* **2016**, 026 (2016), arXiv:1511.00014 [astro-ph.HE].
- [23] Y.-F. Liang, Z.-Q. Shen, X. Li, Y.-Z. Fan, X. Huang, S.-J. Lei, L. Feng, E.-W. Liang, and J. Chang, *Phys. Rev. D* **93**, 103525 (2016), arXiv:1602.06527 [astro-ph.HE].
- [24] Z.-Q. Shen, Z.-Q. Xia, and Y.-Z. Fan, *Astrophys. J.* **920**, 1 (2021), arXiv:2108.00363 [astro-ph.HE].
- [25] Y. Z. Fan, J. Chang, J. H. Guo, Q. Yuan, Y. M. Hu, *et al.*, *Acta Astronomica Sinica* **63**, 27 (2022).
- [26] T. H. Reiprich and H. Böhringer, *Astrophys. J.* **567**, 716 (2002), arXiv:astro-ph/0111285 [astro-ph].
- [27] Y. Chen, T. H. Reiprich, H. Böhringer, Y. Ikebe, and Y. Y. Zhang, *Astron. Astrophys.* **466**, 805 (2007), arXiv:astro-ph/0702482 [astro-ph].
- [28] P. Bruel, T. H. Burnett, S. W. Digel, G. Johannesson, N. Omodei, and M. Wood, *ArXiv e-prints* (2018), arXiv:1810.11394 [astro-ph.IM].
- [29] M. Ackermann, M. Ajello, A. Albert, A. Allafort, *et al.* (Fermi-LAT), *Astrophys. J. Suppl. Ser.* **203**, 4 (2012), arXiv:1206.1896 [astro-ph.IM].
- [30] W. Atwood, A. Albert, L. Baldini, M. Tinivella, *et al.*, *ArXiv e-prints* (2013), arXiv:1303.3514 [astro-ph.IM].
- [31] H. Dembinski and P. O. et al., (2020), 10.5281/zenodo.3949207.
- [32] M. Ackermann, M. Ajello, A. Albert, A. Allafort, *et al.* (Fermi-LAT), *Phys. Rev. D* **88**, 082002 (2013), arXiv:1305.5597 [astro-ph.HE].
- [33] Y. Su, R. P. Kraft, P. E. J. Nulsen, C. Jones, T. J. Maccarone, F. Mernier, L. Lovisari, A. Sheardown, *et al.*, *Astron. J.* **158**, 6 (2019), arXiv:1904.11899 [astro-ph.GA].
- [34] M. A. Sánchez-Conde and F. Prada, *Mon. Not. Roy. Astron. Soc.* **442**, 2271 (2014), arXiv:1312.1729 [astro-ph.CO].
- [35] A. Moliné, M. A. Sánchez-Conde, S. Palomares-Ruiz, and F. Prada, *Mon. Not. Roy. Astron. Soc.* **466**, 4974 (2017), arXiv:1603.04057 [astro-ph.CO].
- [36] T. Ishiyama and S. Ando, *Mon. Not. Roy. Astron. Soc.* **492**, 3662 (2020), arXiv:1907.03642 [astro-ph.CO].
- [37] L. Feng, Y.-F. Liang, T.-K. Dong, and Y.-Z. Fan, *Phys. Rev. D* **94**, 043535 (2016), arXiv:1608.04056 [hep-ph].
- [38] T. Lacroix, G. Facchinetti, J. Pérez-Romero, M. Stref, J. Lavalle, D. Maurin, and M. A. Sánchez-Conde, *JCAP* **10**, 021 (2022), arXiv:2203.16440 [astro-ph.HE].
- [39] F. Aharonian, D. Khangulyan, and D. Malyshev, *Astron. Astrophys.* **547**, A114 (2012), arXiv:1207.0458 [astro-ph.HE].
- [40] J. Chang *et al.* (DAMPE), *Astropart. Phys.* **95**, 6 (2017), arXiv:1706.08453 [astro-ph.IM].
- [41] A. Simionescu, N. Werner, A. Mantz, S. W. Allen, and O. Urban, *Mon. Not. R. Astron. Soc.* **469**, 1476 (2017), arXiv:1704.01236 [astro-ph.CO].
- [42] O. G. Kashibadze, I. D. Karachentsev, and V. E. Karachentseva, *Astron. Astrophys.* **635**, A135 (2020), arXiv:2002.12820 [astro-ph.GA].
- [43] D. Galdeano, G. Coldwell, F. Duplancic, S. Alonso, L. Pereyra, D. Minniti, R. Zelada Bacigalupo, *et al.*, *Astron. Astrophys.* **663**, A158 (2022), arXiv:2205.03424 [astro-ph.GA].
- [44] K.-W. Wong, J. A. Irwin, D. R. Wik, M. Sun, C. L. Sarazin, Y. Fujita, and T. H. Reiprich, *Astrophys. J.* **829**, 49 (2016), arXiv:1602.06950 [astro-ph.HE].
- [45] D. Brout *et al.*, *Astrophys. J.* **938**, 110 (2022), arXiv:2202.04077 [astro-ph.CO].
- [46] S. Abdollahi *et al.* (Fermi-LAT), *Astrophys. J. Supp.* **260**, 53 (2022), arXiv:2201.11184 [astro-ph.HE].
- [47] M. Cirelli, G. Corcella, A. Hektor, G. Hutsi, M. Kadastik, P. Panci, M. Raidal, F. Sala, and A. Strumia, *JCAP* **03**, 051 (2011), [Erratum: *JCAP* 10, E01 (2012)], arXiv:1012.4515 [hep-ph].
- [48] M. Ackermann *et al.* (Fermi-LAT), *Phys. Rev. Lett.* **115**,

- 231301 (2015), arXiv:1503.02641 [astro-ph.HE].
- [49] A. Albert *et al.* (Fermi-LAT, DES), *Astrophys. J.* **834**, 110 (2017), arXiv:1611.03184 [astro-ph.HE].
- [50] J. Conrad, *Astroparticle Physics* **62**, 165 (2015), arXiv:1407.6617 [astro-ph.CO].
- [51] Z.-L. Xu, K.-K. Duan, Z.-Q. Shen, *et al.*, *Res. Astron. Astrophys.* **18**, 027 (2018), arXiv:1712.02939.
- [52] K.-K. Duan, W. Jiang, Y.-F. Liang, *et al.*, *Res. Astron. Astrophys.* **19**, 132 (2019), arXiv:1904.13098.